NREL/CP-520-25628

Large-Signal Injection-Level Spectroscopy of Impurities in Silicon

R.K. Ahrenkiel and S.W. Johnston
National Renewable Energy Laboratory

Presented at the National Center for Photovoltaics Program Review Meeting
Denver, Colorado
September 8-11, 1998

National Renewable Energy Laboratory
1617 Cole Boulevard
Golden, Colorado 80401-3393
A national laboratory of the U.S. Department of Energy
Managed by Midwest Research Institute
for the U.S. Department of Energy
under contract No. DE-AC36-83CH10093

Work performed under task number PV903101

October 1998

NOTICE

This report was prepared as an account of work sponsored by an agency of the United States government. Neither the United States government nor any agency thereof, nor any of their employees, makes any warranty, express or implied, or assumes any legal liability or responsibility for the accuracy, completeness, or usefulness of any information, apparatus, product, or process disclosed, or represents that its use would not infringe privately owned rights. Reference herein to any specific commercial product, process, or service by trade name, trademark, manufacturer, or otherwise does not necessarily constitute or imply its endorsement, recommendation, or favoring by the United States government or any agency thereof. The views and opinions of authors expressed herein do not necessarily state or reflect those of the United States government or any agency thereof.

Available to DOE and DOE contractors from:
Office of Scientific and Technical Information (OSTI)
P.O. Box 62
Oak Ridge, TN 37831
Prices available by calling 423-576-8401

Available to the public from:
National Technical Information Service (NTIS)
U.S. Department of Commerce
5285 Port Royal Road
Springfield, VA 22161
703-605-6000 or 800-553-6847
or
DOE Information Bridge
http://www.doe.gov/bridge/home.html

Printed on paper containing at least 50% wastepaper, including 10% postconsumer waste

Large-Signal Injection-Level Spectroscopy of Impurities in Silicon

R.K. Ahrenkiel and S.W. Johnston

National Renewable Energy Laboratory
Golden, CO 80401

ABSTRACT. Deep level defects in silicon are identified by measuring the recombination lifetime as a function of the injection level. The basic models for recombination at deep and shallow centers is developed. The defect used for the theoretical model is the well-known interstitial Fe ion in silicon. Data are presented on silicon samples ranging in defect content from intentionally Fe-doped samples to an ultra-pure float-zone grown sample. These data are analyzed in terms of the injection-level spectroscopy model.

INTRODUCTION

The identification of semiconductor defects is a major task in the photovoltaic technology. A *contactless* technique that is an impurity diagnostic is especially desirable. We have found a new technique that measures the recombination lifetime over a wide range of injection levels and is a sensitive technique for material characterization. Primarily, this technique measures the minority-carrier lifetime, a most important parameter of device performance. As a spin-off benefit, we can sometimes identify the defect by observing the details of the excess carrier decay over several orders of magnitude. This novel characterization and identification method will be the focus of this work.

The Shockley-Read-Hall (SRH) process is perhaps the most prevalent recombination mechanism in the class of flat-plate, low-cost photovoltaic (PV) devices. The trade-off between material purity and production cost results in a compromise in impurity and defect content. The result of this compromise is that most flat plate solar cells are SRH-imited. The injection-level (ILS) spectroscopy technique provides the important lifetime parameter. In addition, the identity of the dominant defect can also be learned from the measurement.

Recombination physics

One can show that the SRH recombination rate at low and high injection is a function of the defect electron and hole capture cross-sections. The SRH rate is also a function of the defect energy level in the forbidden gap. The Shockley-Read-Hall recombination mechanism is related to defects such as chemical impurities, mechanical defects, and grain boundaries. One can separate the SRH defects into surface and bulk defects. The surface component can be written in terms of a surface recombination velocity S. For a wafer of thickness d, the total SRH lifetime is written as:

$$\frac{1}{\tau_{SRH}} = \frac{1}{\tau_B} + \frac{2S}{d}. \qquad 1)$$

where τ_B is the bulk lifetime and d is the wafer thickness.

The SRH Effect as a Function of Injection

The SRH recombination rate produced by a single point defect at energy E_t in the forbidden gap is described by the well-known equation [1,2]:

$$\frac{dn}{dt} = \frac{dp}{dt} = -\frac{\sigma_p \sigma_n v_{th} N_t \left(pn - n_i^2\right)}{\sigma_n\left[n + n_i \exp\left(\frac{E_t - E_i}{kT}\right)\right] + \sigma_p\left[p + n_i \exp\left(\frac{E_i - E_t}{kT}\right)\right]}. \quad 2)$$

Here, n and p are the densities of free electrons and holes, respectively, and N_t is the defect density. Also, σ_n and σ_p are the capture cross-sections for electrons and holes, respectively. Finally, v_{th} is the thermal velocity, n_i is the intrinsic density, and E_i is intrinsic energy. The SRH lifetime is not a single number, but is a function of the electron and hole concentrations.

In p-type material, we substituted for n and p in terms of the excess carrier density. The recombination rate is then written as:

$$\frac{d\rho}{dt} = -\frac{\sigma_p \sigma_n v_{th} N_t \left(\rho N_A + \rho^2\right)}{\sigma_n\left(\rho + n_i \exp\left(\frac{E_t - E_i}{kT}\right)\right) + \sigma_p\left(N_A + \rho + n_i \exp\left(\frac{E_i - E_t}{kT}\right)\right)}. \quad 3)$$

where $\rho = \Delta n = \Delta p$, the density of light-generated electron-hole pairs, respectively. We also call ρ the excess carrier density.

In summary, the SRH lifetime is a function of the injection level. At low injection ($\rho < N_A$), and when $E_t \sim E_i$, the lifetime from Eq. 3 is:

$$\tau_{low} = \frac{1}{\sigma_n N_t v_{th}}. \quad 4)$$

At high injection ($\rho > N_A$), the *recombination or high-injection lifetime* is:

$$\tau_{high} = \frac{1}{\sigma_p N_t v_{th}} + \frac{1}{\sigma_n N_t v_{th}}. \quad 5)$$

Eqs. 4 and 5 are the asymptotic limits of the recombination rate given by Eq. 3. For a single deep level, one can measure these SRH lifetimes at the extremes of injection level. The ratio of the high-injection to low-injection lifetime is:

$$\text{ratio} = \frac{\sigma_n + \sigma_p}{\sigma_p}. \quad 6)$$

The ratio is a number that is impurity specific and is the basis of injection-level spectroscopy.

Small-signal Lifetime

We will define the *small-signal lifetime* as the inverse of the logarithmic derivative of $\rho(t)$ at a specific value of ρ.

$$\frac{1}{\rho}\frac{d\rho}{dt} = -\frac{1}{\tau} = -\frac{(N_A + \rho)}{\tau_p\left(\rho + n_i \exp\left(\frac{E_t - E_i}{kT}\right)\right) + \tau_n\left(N_A + \rho + n_i \exp\left(\frac{E_i - E_t}{kT}\right)\right)}. \qquad 7)$$

$$\text{where } \tau_p = \frac{1}{\sigma_p N_t v_{th}},$$

$$\text{and } \tau_n = \frac{1}{\sigma_n N_t v_{th}}.$$

Now, by inverting Eq. 7, the small-signal lifetime is:

$$\tau = \frac{\tau_p\left[\rho + n_i \exp\left(\frac{E_t - E_i}{kT}\right)\right] + \tau_n\left[N_A + \rho + n_i \exp\left(\frac{E_i - E_t}{kT}\right)\right]}{\rho + N_A}. \qquad 8)$$

The measurement apparatus usually operates by injecting some test signal ρ (excess carriers) into the sample and recording the decay as ρ approaches zero. If a steady-state light bias produces the excess carrier density ρ, and a small test signal produces an increment $\Delta\rho$, the lifetime vs. ρ can be mapped from Eq. 8.

ILS Theory

A Model Deep Impurity: Interstitial Fe in Silicon

As an example of this injection-dependent lifetime, let us calculate lifetimes of silicon wafers controlled by some common iron-related defects. The electron and hole capture cross-sections of interstitial iron (Fe_i^+) are presented in the literature [3,4]:

$$\sigma_n = 2 - 3.5 \times 10^{-14}\ \text{cm}^2$$
$$\sigma_p = 2 - 3.0 \times 10^{-16}\ \text{cm}^2 \qquad 9)$$

The Coulomb force produces an electron capture cross-section that is about 100 times larger than the hole cross-section. The Fe_i ion produces a deep donor level that lies at 0.43 eV above the valence band and has a Coulomb attraction for electrons. In n-type silicon, the center is a neutral trap for holes.

We will define the injection level, I, as:

$$I = \rho/N. \qquad 10)$$

In Fig. 1, the small-signal lifetime is plotted with parameters $N_t = N_{Fei} = 1 \times 10^{12}$ cm^{-3}, T = 290 K, using three p-type and one n-type doping levels. The range of injected carriers, ρ, used in the calculation varies from $\rho = 1 \times 10^{10}$ cm^{-3} to 1×10^{16} cm^{-3}. Curve A shows the calculated results with the hole density p equal to 1×10^{14} cm^{-3}. A lifetime of 1.5 µs is seen at low-injection levels (below about 1×10^{11} cm^{-3}). At an injection density of 1×10^{12} cm^{-3}, we see that the instantaneous lifetime has increased to 3.0 µs. This corresponds to an injection level I of 0.01. Therefore, experimentalists must be very careful in assuming low injection. Achieving low injection is especially difficult when there is a large cross-section ratio, as is the case for Fe_i. Curves B and C correspond to p-type carrier concentrations of 1×10^{13} cm^{-3} and 1×10^{12} cm^{-3}, respectively. We show that decreasing the p-type doping density merely shifts the decay curve to lower injection levels. Curve D is calculated with n-type doping of 1×10^{12} cm^{-3} and is independent of injection level. A generalized form for the lifetime ratio can be written from Eq. 6:

$$\text{ratio} = \frac{\sigma_{min} + \sigma_{maj}}{\sigma_{maj}}. \qquad 11)$$

For these data, we find a value of 1.01 indicating that $\sigma_{maj} \approx 100\ \sigma_{min}$. In general, an SRH response that is independent of injection level, indicates that the minority-carrier cross-section is much smaller than the majority-carrier cross-section. This is the case for the Fe_i ion in n-type silicon.

Large-signal Excess Carrier Decay

If a technique with large dynamic range is available, one can obtain $\rho(t)$ over several decades in a single measurement. The time-resolved photoluminescence technique has been successfully used in this mode [5] but does not work for indirect bandgap materials such as silicon. In this paper, we will show that the ultra-high frequency photoconductive decay (UHFPCD) technique is applicable for ILS measurements in indirect bandgap materials such as silicon. In the ILS applications, these can be defined as large-signal injection-level spectroscopy (LSILS) techniques.

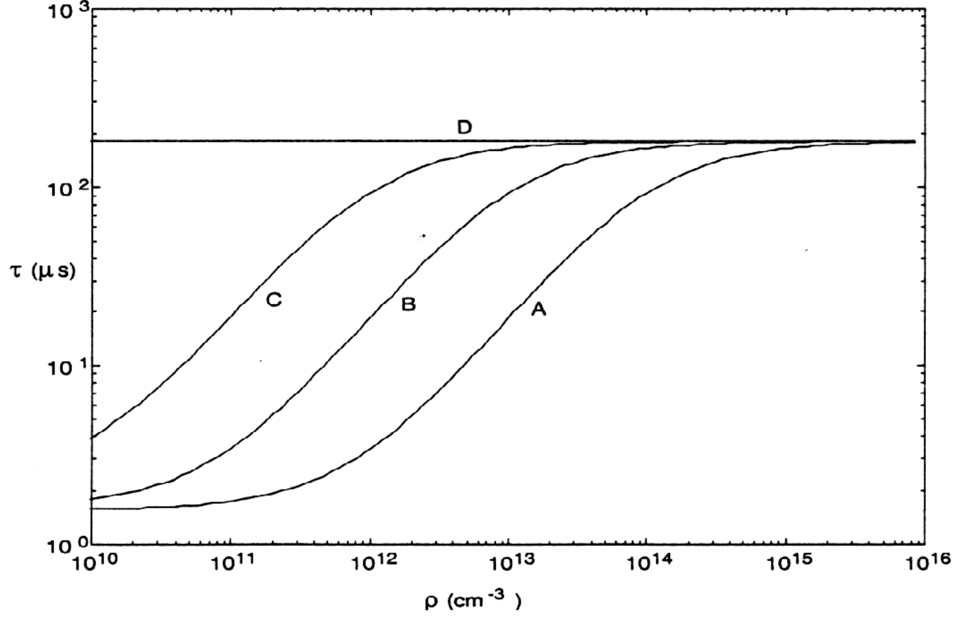

Fig. 1. The calculated lifetime resulting from interstitial Fe impurities in silicon. Curve A: Fe_i ion density = 1 x 10^{12} cm^{-3} for all curves. A: p= 1 x 10^{14} cm^{-3}; B: p=1 x 10^{13} cm^{-3}; C: p = 1 x 10^{12} cm^{-3}; D:n= 1 x 10^{12} cm^{-3}.

Large signal excess carrier decay of the Fei center.

As an example, we have calculated the transient behavior of excess-carrier densities for the Fe_i recombination center. The calculations were performed by numerically integrating Eq. 2 over various time periods, thereby obtaining ρ(t). Eq. 2 can be solved numerically using the Runge-Kutta algorithm and all of these calculations ignore surface recombination contribution.

We assumed an Fe_i density of 1 x 10^{12} cm^{-3} and a hole concentration of 1 x 10^{14} cm^{-3} to calculate ρ(t) for all calculations. We calculated ρ(t) for five initial injected carrier densities and show the results in Fig. 2. The injected carrier densities, ρ(t=0), can be read from the intercept with the ρ axis at t=0. Curve A represents the decay with an injection density of 1 x 10^{10} cm^{-3}, and the low-injection lifetime of 1.53 μs occurs for the entire decay. Curve B represents an injection density of 1 x 10^{12} cm^{-3} and the initial lifetime increased to 3.25 μs. The low-injection lifetime of 1.53 μs is seen when the excess carrier density is less than about 1 x 10^{11} cm^{-3}. Curve C (ρ_0 = 1 x 10^{13} cm^{-3}) has an initial lifetime of 17.5 μs, whereas Curve D, with ρ = 5 x 10^{13} cm^{-3} has τ (0) = 59.4 μs. Curve E, which represents I=1.0, has τ (0) = 87.3 μs. We do not reach the high-injection lifetime of 177 μs in these calculations. Our results show that the low-injection lifetime requires $\rho < 1 \times 10^{11}$ cm^{-3}. This result contradicts the often-used assumption that low injection is reached when $\rho < N_A$. For this particular recombination center, low

injection requires that $\rho < 0.01\ N_A$. In the laboratory, one must be very judicious in assigning low-injection values to a particular measurement.

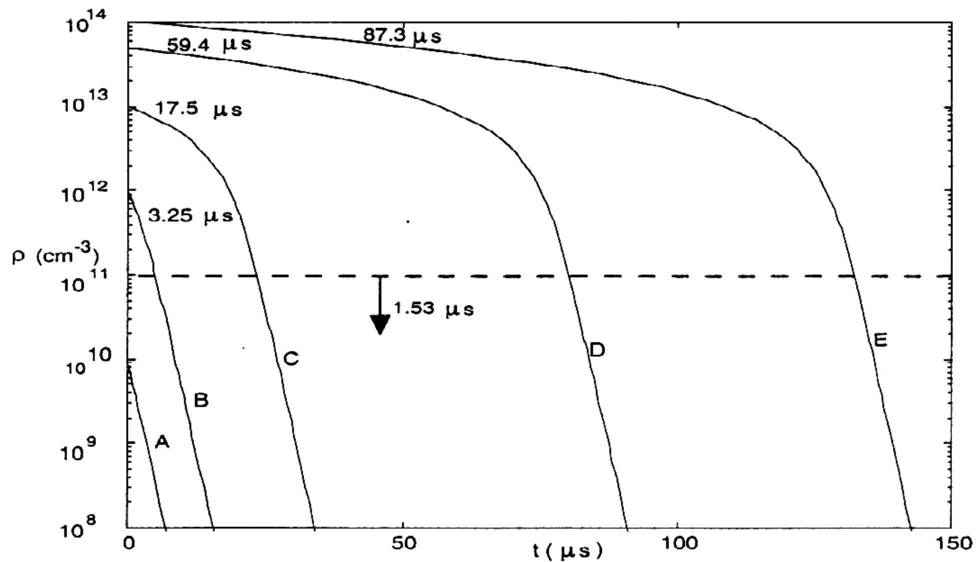

Fig. 2. The calculated large-signal excess carrier decay density versus time with injection levels ranging from 1 x 10^{12} cm^{-3} to 1 x 10^{16} cm^{-3} for a silicon sample with 1 x 10^{12} cm^{-3} Fe_i ions. The p-type doping is also 1 x 10^{14} cm^{-3}. Curves A through E represent five initial injection levels indicated by the intercept with the ρ axis.

MEASUREMENT TECHNIQUES

Photoconductive Decay

The measurement of recombination lifetimes in silicon have predominately used some form of photoconductive decay (PCD). Most PCD techniques use a pulsed light source to produce a transient increase in conductivity. The photoconductive transient, $\Delta\sigma$, decays with the excess carrier density. Prior to the last decade, photoconductive lifetime measurements were commonly made by combining a two- or four-point probe system [6] with a pulsed light source that produced the transient $\Delta\sigma$. Time-resolved microwave conductivity (TRMC) was reported as a lifetime diagnostic quite early[7]. In 1959, Mada [8] used TRMC to produce lifetime maps of silicon wafers. This technique has been further developed by numerous workers in the field of silicon characterization.

Time-resolved Microwave Conductivity

Within the last 10 years, TRMC has become the most popular technique of the silicon-related technologies because it is contactless and nondestructive. Nonlinearity is one of the inherent limitations of TRMC, and only small-signal measurements of $\Delta\sigma/\sigma$ are meaningful. Kunst and Beck [9] calculated the microwave reflectance of a thick

semiconducting medium at microwave frequencies. The calculations show that the reflectivity is about 1.0 near conductivities of 0.01 ohm^{-1} cm^{-1}. The reflectivity decreases to about 0.75 at 1.0 ohm^{-1} cm^{-1} and then increases to about 0.9 at 10 ohm^{-1} cm^{-1}. Therefore, TRMC is not usually suitable for large-signal injection-level spectroscopy. Injection-level measurements are made by combining a dc bias light source to produce a steady-state level (ρ) and a weaker pulsed source to measure the small-signal lifetime (Δρ). In this manner, the small-signal lifetime can be mapped over a range of injection levels.

Ultra-high Frequency Photoconductive Decay

The ultra-high-frequency photoconductive technique[10,11,12,13,14] was shown to be linear in excess conductivity over several orders of magnitude. The principle of operation uses photo-induced eddy currents driven at ultra-high frequencies (420 to 430 MHz). We will describe large-signal injection-level spectroscopy experiments on various types of silicon. Our apparatus is linear in Δσ over more than three orders of magnitude. Our discussion here will describe using UHFPCD for defect identification in samples ranging from ultra-high purity to heavily contaminated silicon.

EXPERIMENTAL DATA

Fe-ion in n-type Silicon

Lifetime data for a float-zone crystal heavily doped with iron is first presented. The target doping for this crystal was 1×10^{15} cm^{-3}, but, because of clustering, the actual point-defect density is much lower [15]. No shallow dopants were added during growth. Our resistivity measurements indicate that $n = 1.7 \times 10^{13}$ cm^{-3}, and therefore, the Fermi level is about 0.18 eV above midgap. The isolated Fe intersitial ion is a deep donor lying 0.4 eV above the valence band. As the Fermi level "pins" near the deep level, a donor state of the Fe complex must be active here. The active donor level must lie much higher to produce this carrier concentration. A deep donor (Ec - 0.41 eV) and several deep acceptors states have been observed using deep-level transient spectroscopy (DLTS) [9, 10] in heavily-Fe-doped silicon. Kitagawa and coworkers were able to disassociate the deep donor center by annealing.

Fig. 3 shows the injection-level dependence of the lifetime of this sample. The low-injection lifetime, Curve A, is 1.12 µs. Upon increasing the injection level (Curve B), the graph shows negative curvature of a deep level, with an initial lifetime of 5.17 µs. Finally, the high-injection lifetime saturates at 66 µs as shown in Curve C. These data are very similar in character to the model calculations of Fig. 3 except that they indicate a large σ_p/σ_n ratio. The recombination center, in this case, is one of the deep acceptor Fe-complexes. However, these data point out the basic overall agreement with the SRH model.

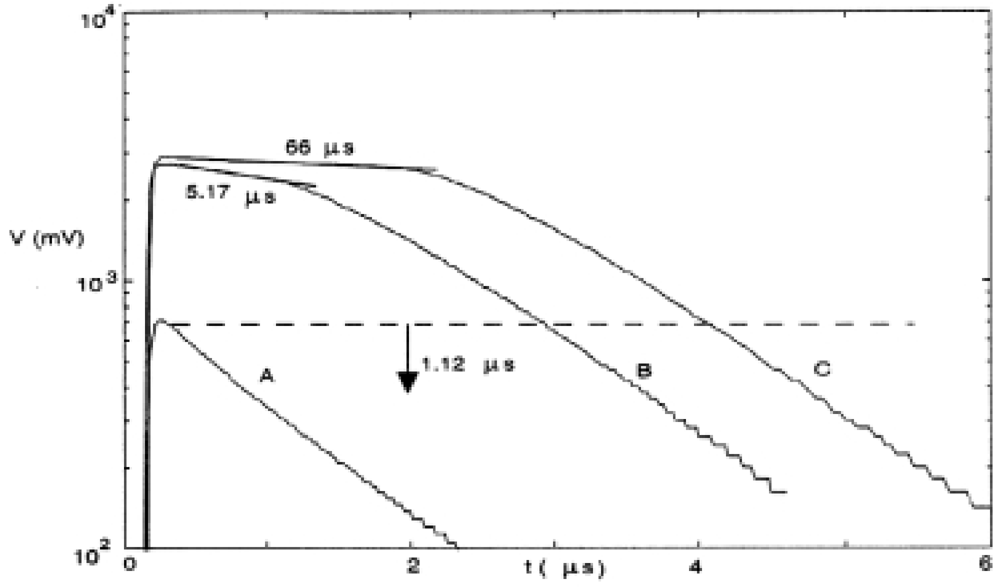

Fig. 3 The UHFPCD data for a float-zone silicon sample that is doped with Fe to over 1 x 10^{14} cm^{-3}. Curves A, B, and C were taken at increasing injection levels. The instantaneous lifetimes are indicated on the figure.

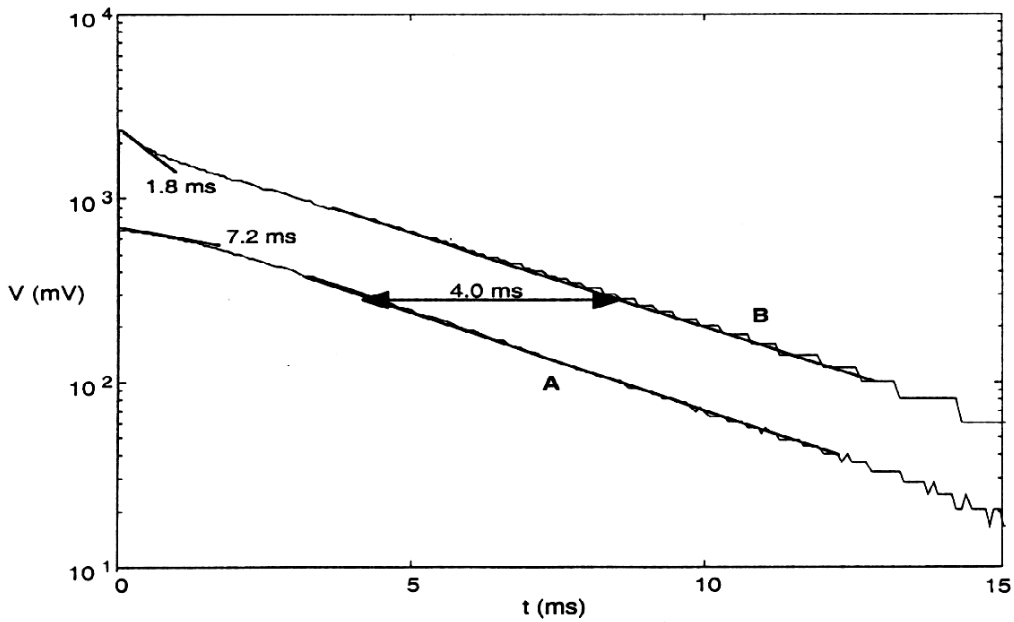

Fig. 4. The UHFPCD data for a wafer of high-purity float-zone silicon. Curves A and B represent two injection levels. The instantaneous lifetimes are indicated.

High-purity Float-zone Silicon

To show other decay patterns, we present some data on high-purity, high-resistivity float-zone wafers supplied by Unisil Corporation. These samples are n-type wafers with resistivities in the 4500 to 6500 Ω-cm range. The surface recombination velocity S becomes very important for these samples because of the expected weak volume-recombination rate. Consequently, these wafers were etched in hydroflouric acid (HF), rinsed in deionized water, and placed in a saturated iodine/methanol (I/M) solution. The I/M treatment reduces the surface recombination velocity to very low values [16].

The UHFPCD data for one of the better samples are shown in Fig. 4. The light source is a highly attenuated YAG laser operating at 1064-nm wavelength. Two injection levels are shown by Curves A and B. Curve A shows a decay that is constant at about 4.0 ms over about two decades of injection level. There is a weak high-injection plateau at the initial portion of the decay, with a lifetime of 7.2 ms. Increasing the injection level, Curve B shows that the slope decreases at $t = 0$, rather than increasing the high-injection portion of the curve. The initial decay can be understood in terms of the injection-activated Auger effect. The long-term decay behavior is consistent with a low density of neutral SRH defects that lie near midgap. A large injection level is required to "fill" the centers with minority carriers. Using the value of 1.8 ms and known Auger coefficients, this portion of the curve can be fit to an injected carrier density of 4.4×10^{16} cm^{-3}. This value is very compatible with calculations of the absorbed laser photons.

CONCLUSIONS

We have shown the application of the theory of SRH recombination in real-time excess carrier decay. We have developed the ILS theory for modeling deep and shallow recombination centers. Our lifetime measurement apparatus has a large dynamic range, so that the excess carrier density ρ can be measured over at least two decades. As the database for defect identification increases, the ILS technique will become more useful.

ACKNOWLEDGEMENTS

The authors would like to thank T. Wang for supplying the Fe-doped silicon wafers and K. Smith of Unisil for supplying the high-purity float-zone wafers. The authors would like to thank B. M. Keyes and S. P. Ahrenkiel for a critical reading of the manuscript. This work was supported by the U. S. Department of Energy under Contract No. DE-AC36-83CH10093.

REFERENCES

1. W. Shockley, and W. T. Read, Phys. Rev. **87**, 335, (1952) .
2. R. N. Hall, Phys. Rev. **87**, 387 1952).
3. H. Daio, K. Yakushijib, A. Buckzkowski, and F. Shimura, Materials Science Forum 196-201, p. 1817, (1995) Trans Tech Publications, Switzerland.
4. A. L. P. Rotondar, T. Q. Hurd, A. Kaniava, J. Vanhellemont, E. Simoen, M. M. Heyns, and C. Claeys, J. Electrochem. Soc. Vol. **143**, 3014 (1996).
5. R. K. Ahrenkiel, B. M. Keyes, and D. J. Dunlavy, J. Appl. Phys. **70**, 225, (1991).
6. D. T. Stevenson and R. J. Keyes, J. Appl. Phys. **26**, 190 (1955).
7. A. P. Ramsa, H. Jacobs, and F. A. Brand, J. Appl. Phys. **39**, 1054 (1959).
8. Y. Mada, Japan. J. Appl. Phys. **18**, 2171 (1979).
9. M. Kunst and G. Beck, J. Appl. Phys. **60**, 3558 (1986).
10. R. K. Ahrenkiel, AIP Conference Proceedings **353**, p161, AIP Press (1996).
11. R.K. Ahrenkiel, AIP Conference Proceedings **394**, p. 225, AIP Press, (1997).
12. R. K. Ahrenkiel and S. Johnston, Mat. Res. Soc. Symp. Proc. Vol. **510**,p. 575-581, Materials Research Society (1998).
13. R. K. Ahrenkiel and S. Johnston, Solar Cells and Solar Energy Materials **55**, 59 (1998).
14. R. K. Ahrenkiel and S. Johnston, Proceedings of the 26th Photovoltaic Specialists Conference,1997, p. 119, IEEE Press, 1998 .
15. T. F. Ciszek, T. H. Wang, R. K. Ahrenkiel, and R. Matson, Twenty-Fifth IEEE Photovoltaic Specialists Conference,1996, p. 737 (1996).
16. H. M'Saad, G. J. Norga, J. Michel, and L. C. Kimmerling, AIP Conference Proceedings **306**, 471 (1994). American Institute of Physics Press, New York, R. Noufi and H. Ullal, eds.